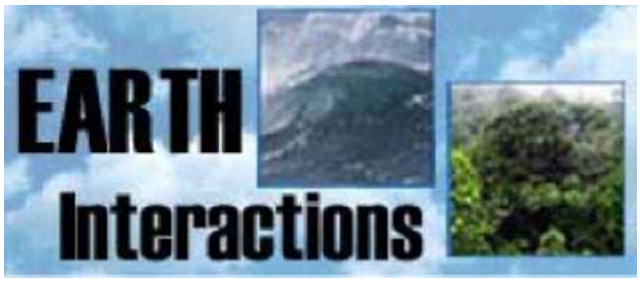

Multitemporal Analysis of Degraded Forests in the Southern Brazilian Amazon

Carlos M. Souza Jr.*

Instituto do Homem e Meio Ambiente da Amazônia—Imazon, Belém, Pará, Brazil, and Department of Geography, University of California, Santa Barbara, Santa Barbara, California

Dar A. Roberts

Department of Geography, University of California, Santa Barbara, Santa Barbara, California

André L. Monteiro

Instituto do Homem e Meio Ambiente da Amazônia—Imazon, Belém, Pará, Brazil

Received 14 September 2004; accepted 9 February 2005

ABSTRACT: In this study, statistical multitemporal analysis was applied to evaluate the capability of reflectance, vegetation indices [normalized difference vegetation index (NDVI) and soil adjusted vegetation index (SAVI)], normalized difference infrared indices (NDII5 and NDII7), and fraction images, derived from spectral mixture analysis (SMA), to distinguish intact forest from four classes of degraded forests: nonmechanized logging, managed logging,

* Corresponding author address: Carlos Souza Jr., Instituto do Homem e Meio Ambiente da Amazônia—Imazon, Caixa Postal 5101, Belém, Pará 66613-397, Brazil.
E-mail address: souzajr@imazon.org.br

conventional logging, and logged and burned. For this purpose, a robust time series dataset of Landsat Thematic Mapper 5/Enhanced Thematic Mapper (TM/ETM+) images was used in conjunction with forest inventory transects and data on disturbance history. The study area is located near two important sawmill centers—Sinop and Claúdia, in Mato Grosso State—in the southern Brazilian Amazon. Most of the remote sensing measures tested to distinguish intact forest from degraded forests showed statistically significant changes. Fraction images, particularly green vegetation (GV) and nonphotosynthetic vegetation (NPV), were the most effective means tested for identifying conventional logging and logged and burned forest in the region. The GV change, detected from intact forest to conventional logging and logged and burned forest classes, persists no more than 1 yr, but the NPV change is still significantly different for up to 2 yr. In the second and third years following a degradation event, a significant regeneration change signal was observed in reflectance and fraction images, which can be useful for identifying these types of forest disturbances in areas where optical satellite images cannot be acquired every year.

KEYWORDS: Forest degradation; Spectral mixture analysis; Brazilian Amazon

1. Introduction

Selective logging, fragmentation, and forest burning are the main factors contributing to forest degradation of the Brazilian Amazon. The major impacts of these anthropogenic disturbances include decreasing forest biomass (Cochrane and Schulze 1999; Gerwing 2002), creating favorable environments for nonnative species (Vidal et al. 1997), and causing local species extinctions (Martini et al. 1994). It has been estimated through field surveys and socioeconomic interviews that up to 10 000–15 000 km^2 are logged, 80 000 km^2 are burned, and 38 000 km^2 are fragmented each year (Nepstad et al. 1999), making the area affected by forest degradation much larger than the area deforested annually in the Amazon, which averages around 18 000 km^2 yr^{-1} (INPE 2003).

Several methodologies have been developed for mapping selective logging and burned forests in the Brazilian Amazon using multispectral satellite images. Examples include visual interpretation (Watrin and Rocha 1992), supervised classification (Stone and Lefebvre 1998), soil fraction images obtained through spectral mixture analysis (Souza and Barreto 2000; Monteiro et al. 2003), contextual clustering (Sgrenzaroli et al. 2002), and decision tree classification (Souza et al. 2003). Additionally, efforts have been made to link forest biophysical properties of selectively logged forests with remotely sensed data (Asner et al. 2002; Asner et al. 2004). Burned forests have also been successfully mapped with nonphotosynthetic vegetation (NPV) fraction images in the eastern Amazon (Cochrane and Souza 1998).

To date, few studies have employed multitemporal data to map forest degradation, which has been considered an important attribute for monitoring tropical forests (Lambin 1999). Single-date or infrequent satellite acquisitions represent a potential source of error due to rapid canopy closure and regeneration of degraded forest, leading to misclassification of degraded forests as intact (Stone and Lefebvre 1998). Furthermore, while several authors have used at least two dates to

characterize selectively logged forests (Stone and Lefebvre 1998; Souza and Barreto 2000; Monteiro et al. 2003; Asner et al. 2002), the same types of temporal analysis have not been applied to characterize burned forest dynamics. Currently, no study that we are aware of has used high temporal frequency images (i.e., at least one per year) to characterize change dynamics of the full range of forest degradation classes existing in the Amazon region. As a result, the optimal temporal resolution for mapping degraded forests has yet to be determined. In this study, we seek to contribute to an understanding of the temporal dynamics of degraded forests. Specifically, we wish to answer two main questions. 1) How long do the degraded forest "signatures" persist on Landsat images? 2) And what is the optimal temporal resolution for mapping degraded forests with Landsat images? To answer these questions, we evaluated changes in reflectance, vegetation, and infrared indices and fraction images derived from spectral mixture analysis over a chronosequence of well-characterized degraded forest types. Image analysis utilized a robust time series dataset of Landsat Thematic Mapper 5/Enhanced Thematic Mapper (TM/ETM+) images, encompassing 20 yr of images acquired for every year. Field data included 19 forest transect inventories covering all types of degraded forests found in the study area.

2. Study area and forest degradation patterns

The study area is located in the state of Mato Grosso, Brazil, in the vicinity of the Sinop and Cláudia sawmill centers (Figure 1). Transitional forest, between cerrado and dense forest, is the predominant vegetation type in the region. The topography varies from flat to undulating terrain, on latosol soils, and the average annual precipitation is 2000 mm (RADAMBRASIL 1981).

Selective logging in this area is characterized by the harvesting of high quality timber species. The harvesting intensity ranges from 10 to 40 m^3 ha^{-1} and is predominantly unplanned (Monteiro et al. 2004). Three types of selectively logged forest were identified in the field: nonmechanized logging, managed logging, and conventional logging forests (Table 1). At the field scale, logged forests are composed of three main environments: 1) forest islands that were not disturbed because of poor access due to topography and rivers, or due to the lack of commercial timber species; 2) areas where the forest had been cleared to create roads for machine movements (skidders and trucks) and log landings to store the harvested timber; and 3) canopy-damaged forests (i.e., harvested areas and areas damaged by tree falls and machine movements). This pattern is similar to the logging pattern found in dense forest areas in the eastern Amazon (Veríssimo et al. 1992; Johns et al. 1996), differing only in the harvesting intensity (30–40 m^3 ha^{-1}).

Forest burning is also frequent in this region, acting synergistically with selective logging to increase forest degradation damages (Monteiro et al. 2004). Selectively logged forests can burn when agricultural fires escape unintentionally from adjacent areas. Prolonged "forest surface fires" eventually reach the heat tolerance of trees and lianas, which can lead to tree mortality (Holdsworth and Uhl 1997; Cochrane and Shultz 1999). As a result, the forests become more degraded and more fuel is accumulated on the forest floor (Cochrane et al. 1999). A second forest surface fire event will likely burn the forest floor more severely and kill more trees (Table 1).

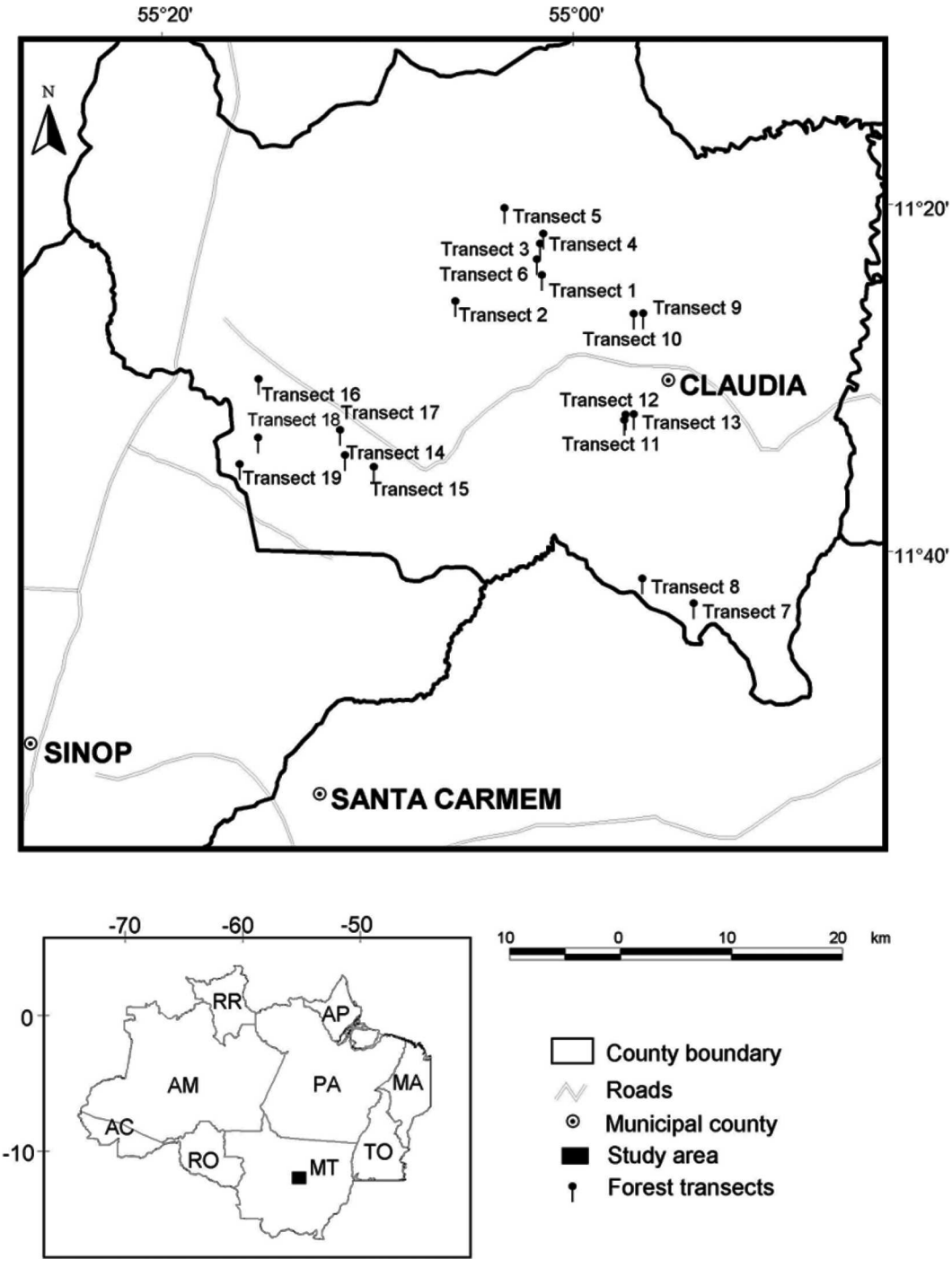

Figure 1. Map of the study area showing the location of the forest transects used to extract satellite pixel data.

Table 1. Characterization of the forest classes defined at the field scale.

Forest class	Field description
Intact	Mature and undisturbed forest.
Nonmechanized logging	Selectively logged forest without the use of vehicles such as skidders and trucks, also known as traditional logging. Log landings, roads, and skid trails are not built.
Managed logging	Planned selective logging where the tree inventory is conducted, followed by road and log landing planning to reduce harvesting impacts.
Conventional logging	Conventional unplanned selective logging using skidders and trucks. Log landings, roads, and skid trails are built.
Logged and burned	Selectively logged forests that have subsequently been damaged by intense surface fires.

3. Dataset

3.1. Satellite imagery data

Eighteen Landsat TM images and three ETM+ images, acquired between 1984 and July 2004, were used in this study (Table 2). The images were acquired through the Tropical Rain Forest Information Center (TRFIC) and the Brazilian Space Agency (INPE).

3.2. Forest transect inventory

Nineteen forest transect inventories were conducted in the study area (Figure 1; Table 3). For the purposes of this study, information about logging and fire

Table 2. Landsat TM/ETM+ data used in this study (orbit/point = 226/068).

Year	Landsat sensor	Day and month	Source
1984	TM5	14 Jun	INPE
1985	TM5	3 Jul	INPE
1986	TM5	7 Aug	INPE
1987	TM5	25 Jun	INPE
1988	TM5	11 Aug	INPE
1989	TM5	31 Aug	INPE
1990	TM5	2 Aug	INPE
1991	TM5	2 Jul	INPE
1992	TM5	25 Jul	INPE
1993	TM5	26 Aug	INPE
1994	TM5	2 Jul	INPE
1995	TM5	13 Jun	INPE
1996	TM5	1 Jul	TRFIC
1997	TM5	5 Aug	INPE
1998	TM5	6 Jun	INPE
1999	ETM+	19 Aug	TRFIC
2000	TM5	26 Jun	INPE
2001	ETM+	8 Aug	INPE
2002	ETM+	10 Jul	INPE
2003	TM5	6 Aug	INPE
2004	TM5	5 Jun	INPE

Table 3. Classification and disturbance history of the forest transects of the study area.

Class	Transect No.	Latitude	Longitude	Time since first logged (years)	Time since last logged (years)	No. of times logged	Volume harvested (m^3 ha^{-1})	No. of times burned
Intact	11	−11.546 110	−54.933 040	—	—	—	—	—
Intact	12	−11.540 960	−54.931 850	—	—	—	—	—
Intact	13	−11.540 550	−54.923 930	—	—	—	—	—
Intact	14	−11.579 852	−55.200 937	—	—	—	—	—
Nonmechanized logging	1	−11.407 170	−55.011 950	2	2	1	10	—
Nonmechanized logging	2	−11.432 190	−55.095 040	5	5	1	10	—
Nonmechanized logging	6	−11.391 950	−55.016 940	2	2	1	10	—
Nonmechanized logging	9	−11.443 970	−54.924 020	11	10	2	25	—
Nonmechanized logging	10	−11.443 660	−54.914 810	14	10	2	25	—
Managed logging	15	−11.591 067 4	−55.173 085 0	4	4	1	38	—
Managed logging	16	−11.506 861 8	−55.283 894 4	3	3	1	32	—
Managed logging	17	−11.555 747	−55.205 766	2	2	1	40	—
Managed logging	18	−11.562 731	−55.284 380	1	1	1	40	—
Managed logging	19	−11.588 599	−55.302 101	0	0	1	25	—
Conventional logging	7	−11.721 690	−54.866 760	4	4	1	10	—
Conventional logging	8	−11.697 990	−54.915 840	8	8	1	10	—
Logged and burned	3	−11.367 190	−55.010 760	2	2	1	25	1
Logged and burned	4	−11.376 690	−55.013 770	2	2	1	25	1
Logged and burned	5	−11.342 810	−55.047 980	4	4	1	25	1

histories, ground cover, canopy cover, and biomass was used to classify the forest degradation classes found at the field scale into four degradation classes: nonmechanized logging, managed logging, conventional logging, and logged and burned (Tables 1 and 3). The forest inventories were conducted following the field protocol proposed by Gerwing (Gerwing 2002) to characterize degraded forest in the eastern Amazon. This method has been successfully applied to characterize biophysical properties and dynamics of degraded forests in transitional forests (Monteiro et al. 2004).

We mapped all trees with diameter at breast height (DBH) greater than 10 cm along a 10 m × 500 m transect. In addition, 10 subparcels (10 m × 10 m) were created every 50 m along each transect. All trees where mapped within the subparcels, and ground cover and canopy cover were estimated. Above-ground biomass was estimated using allometric equations available in the literature (Gerwing 2002; Monteiro et al. 2004), adapted specifically by Gerwing (Gerwing 2002) for degraded forests and estimating vine biomass.

4. Methodology

4.1. Preprocessing: Image registration, atmospheric correction, and intercalibration

The images were registered and radiometrically intercalibrated in order to allow the detection of forest change over time. The Landsat ETM+ image acquired in

1999 was georeferenced using 25 control points extracted from the National Aeronautics and Space Administration (NASA) GeoCover 2000 Mosaic (https://zulu.ssc.nasa.gov/mrsid/). Next, the 1999 georectified Landsat image was used as the reference image to register the images acquired on the other dates (Table 2). The registration was based on the triangulation algorithm and nearest-neighborhood resampling available in the Environment for Visualizing Images 4.0 software (ENVI; Research Systems, Boulder, Colorado), using at least 14 image control points. The root-mean-square (rms) varied from 0.53 to 0.97, which assures that the changes detected over time were not contaminated by misregistration (Verbyla and Boles 2000).

The Landsat ETM+ image from 1999 was first radiometricaly corrected using the gains and offset provided in the image metafile. Next, an atmospheric correction was performed using Atmospheric Correction Now 4.0 (ACORN; Analytical Imaging & Geophysics, Boulder, Colorado). Visibility and water vapor parameters of the atmospheric correction model were determined by a trial-and-error sensitivity analysis of a dark object reflectance (a lake). The final parameters were estimated when the expected reflectance values of the dark object were found. The fixed water vapor was 40 mm, and image atmosphere visibility was 25 km.

The other images (Table 2) were intercalibrated to the reflectance image using a relative radiometric calibration approach (Roberts et al. 1998; Furby and Campbell 2001). This technique assumes that the atmosphere is uniform over the study area and that invariant ground targets can be found over time. Invariant targets representing forest, second growth, green pasture, bare soil, and water were selected for each image pair formed by the 1999 reference image and an uncalibrated image. A linear regression was estimated using the pixel mean values, extracted from a 3 × 3 pixel area, of the invariant targets for each band. These coefficients normalize the uncalibrated images to the 1999 reference image, converting digital numbers of the uncalibrated images to reflectance.

4.2. End-member selection

Image end members representing vegetation, soil, and NPV were extracted from the reference reflectance image. Shade was assigned zero percent reflectance at all wavelengths. The pixel purity index (PPI), available in ENVI 4.0 (Boardman et al. 1995) was used to identify image end-member candidates. Five image subsets (500 × 500 pixels), representing the variety of land cover types found in the images, were used as input for the PPI algorithm. The PPI result was used to identify the pixel location in the original image and extract the spectral curves of these pixels. The final image end members were selected based on the pixel location in the Landsat reflectance spectra with the aid of an *n*-dimensional visualization tool available in ENVI. The pixels located at the extremes of the data cloud of the Landsat spectral space were selected as candidate end members. The final end members were selected based on the spectral shape and image context (e.g., soil spectra are mostly associated with unpaved roads and NPV with pasture having senesced vegetation).

4.3. Spectral mixing models

Spectral mixture analysis (SMA; Adams et al. 1993) assumes that the image spectra are formed by a linear combination of *n* pure spectra, such that

$$\mathrm{DN}_b = \sum_{i=1}^{n} F_i \, \mathrm{DN}_{i,b} + \varepsilon_b \tag{1}$$

for

$$\sum_{i=1}^{n} F_i = 1, \tag{2}$$

where DN_b is encoded radiance in band b, F_i is the fraction of end member i, $\mathrm{DN}_{i,b}$ is encoded radiance for endmember i in band b, and ε_b is the residual error for each band. The SMA model error is estimated for each image pixel by computing the rms error, given by

$$\mathrm{rms} = (n^{-1} \sum_{b=1}^{n} \varepsilon_b)^{1/2}. \tag{3}$$

Mixture models were applied to each date using the intercalibrated image end members, except the reference image, which was the one used to extract the end members. The mixing model results were evaluated as proposed by Adams et al. (1993). First, the rms images were inspected and models with rms values greater than 5% were discarded from the fraction change analysis. Next, fraction images were evaluated and interpreted in terms of field context and spatial distribution. For example, high abundance of soils is mostly associated with dirt roads and high NPV is usually found in pastures. Finally, the histograms of the fraction images were inspected to quantify the percentage of pixels lying outside the range of 0% to 100% and to evaluate fraction value consistency over time (i.e., intact forest shows approximately stable values over time). Only models with at least 98% of the values within 0% to 100% and those that showed mean fraction value consistency over time were kept. For the models that did not pass one of these tests, new invariant targets were collected to improve the image intercalibration coefficients, and a new SMA model was run until the criterion was reached.

4.4. Vegetation and near-infrared indices

We selected two vegetation indices and two normalized difference infrared indices (NDIIs) for assessing if it was possible to distinguish intact forest from the degraded forest classes. The vegetation indices chosen were the normalized difference vegetation index (NDVI; Rouse et al. 1974) and the soil-adjusted vegetation index (SAVI; Huete 1988). These vegetation indices use reflectance measurements from Landsat band 3 (ρ_{b3}) and band 4 (ρ_{b4}) and are computed with the following equations:

$$\mathrm{NDVI} = (\rho_{\mathrm{b4}} - \rho_{\mathrm{b3}})/(\rho_{\mathrm{b4}} + \rho_{\mathrm{b3}}), \tag{4}$$

$$\mathrm{SAVI} = 1.5(\rho_{\mathrm{b4}} - \rho_{\mathrm{b3}})/(\rho_{\mathrm{b4}} + \rho_{\mathrm{b3}} + 0.5). \tag{5}$$

The NDIIs chosen are the ones proposed by Hunt and Rock (Hunt and Rock 1989) to identify forest disturbances associated with water content. These NDIIs are computed using Landsat band 4 (ρ_{b4}), band 5 (ρ_{b5}), and band 7 (ρ_{b7}) and are given by

$$\mathrm{NDII5} = (\rho_{b4} - \rho_{b5})/(\rho_{b4} + \rho_{b5}), \quad (6)$$

$$\mathrm{NDII7} = (\rho_{b4} - \rho_{b7})/(\rho_{b4} + \rho_{b7}). \quad (7)$$

4.5. Class separability and temporal change analyses

Using the information on logging and fire histories acquired during field research and the Landsat time series, it was possible to identify the date prior to degradation, representing the image condition of intact forest. Next, reflectance and fractions of GV, NPV, shade, and soil were extracted using 30 pixels selected randomly within a buffer region of 5 pixels along each transect. Random pixels located in logging roads and log landings were excluded from the analysis because changes from intact forest to clear cut are relatively easier to identify (Souza and Barreto 2000; Monteiro et al. 2003). Less than 1% of the random pixels were excluded following this criterion. The vegetation and infrared indices were computed using the reflectance values extracted from the 30 randomly selected pixels. This procedure allowed us to build a time series dataset of reflectance, vegetation, and infrared indices and fraction values covering the time prior to degradation (i.e., degradation age equals zero) to up to 4 yr after the event.

The next steps were to perform a class separability and temporal change analyses based on reflectance, vegetation and infrared indices, and fractions variables. We used a Tukey test (Ott 1992), available in the R Language (http://www.r-project.org/) to evaluate if the intact forest and the forest degradation classes could be separated from each other and to define for how long the degradation classes could be distinguished from the intact forest class over a period of 4 yr. The Tukey test was run at a 99% confidence interval ($P < 0.01$).

The Tukey test performs a multicomparison of the population means of the intact forest and degraded forest classes; that is, it tests the mean of a population against the mean of each other population. For the purpose of the class separability analysis, the populations are represented by the data acquired prior to the degradation event representing intact forest, and the year right after degradation representing the degraded forest classes (nonmechanized logging, managed logging, conventional logging, and logged and burned). For the purpose of the temporal statistical analysis, the populations are represented by a time variable, encompassing the year prior to the degradation process (i.e., time $= 0$ means intact forest) up to 4 yr after degradation (time $= 1, \ldots, 4$).

Because the Tukey test requires normally distributed samples, a data transformation was applied when necessary by computing the arcsine of the square root of the data variable (Hogg and Craig 1995, 251–252) prior to statistical analysis. The results of the multicomparison statistical analysis are reported only for the comparison of the year prior to the degradation event against each other year. The Tukey test also allowed us to determine how many years a significant difference between intact forest and the degradation classes persisted over time.

5. Results

5.1. First-year forest degradation separability

Four classes of degraded forests were identified and characterized at the field scale: nonmechanized logging, managed logging, conventional logging, and

logged and burned (Table 1). We compared reflectance, vegetation and infrared indices, and fraction means of intact forest relative to each class of degraded forest, and between the other degraded forest classes. Figures 2 and 3 show the results of the class separability analysis, discussed for each type of dataset below 1 yr after the event (also, time = 1 in Table 4).

5.1.1 Reflectance

Mean spectral reflectance ± one standard deviation is plotted for intact forest and the degradation classes in Figure 2a. Qualitative inspection of these spectra indicates high overlap in the Landsat spectral bands making the distinction of these classes challenging.

Statistically, the Tukey test ($P < 0.01$) revealed that spectral differentiation of managed logging, conventional logging, and logged and burned classes from intact forest was possible in the visible part of the spectrum (bands 1–3) for the year the degradation took place (time = 1; Table 4). Nonmechanized logging, however, showed only a significant change from intact forest in band 1. Overall, the differentiation among the other degraded forest classes was also possible in the visible region, except between nonmechanized and managed logging, which did not show significant change in reflectance in the visible region.

According to the statistical test, it was possible to differentiate intact forest from the degraded forest classes, and between each other degraded forest classes, in the near- and mid-infrared spectral region using one or two bands. Nonmechanized logging could not be distinguished in this part of the spectrum from intact forest. In the infrared region, only managed logging and logged and burned classes showed significant statistical differences from intact forest in bands 3, 4, and 5. Conventional logging class showed a significant difference only in band 5 (Figure 2a; Table 4).

A general trend of increasing the mean forest reflectance (1%–2%) as a function of degradation intensity was observed in the visible part of the spectrum (Figure 3a). In the near-infrared region, band 4 showed a decrease (1%–3%) in mean reflectance as a function of degradation intensity, whereas in the shortwave-infrared mean reflectance increased (1%–3%; Figure 3a).

5.1.2. Vegetation indices

The spectral vegetation indices, which rely on high spectral contrast between red and near-infrared bands, did not differentiate nonmechanized logging from intact forest, because of a high overlap between these classes in these two spectral regions (Figures 2a,b; Table 4). However, managed logging, conventional logging, and logged and burned classes showed a significant difference from intact forest and between each other with NDVI and SAVI (Figure 2b; Table 4). Nonetheless, no significant difference was observed between each degraded forest class.

The infrared indices showed a general decreasing trend as a function of degradation intensity (Figures 2b and 3b). Nonmechanized logging could not be distinguished from intact forest and from the other degraded forest classes. However, managed logging, conventional logging, and logged and burned showed

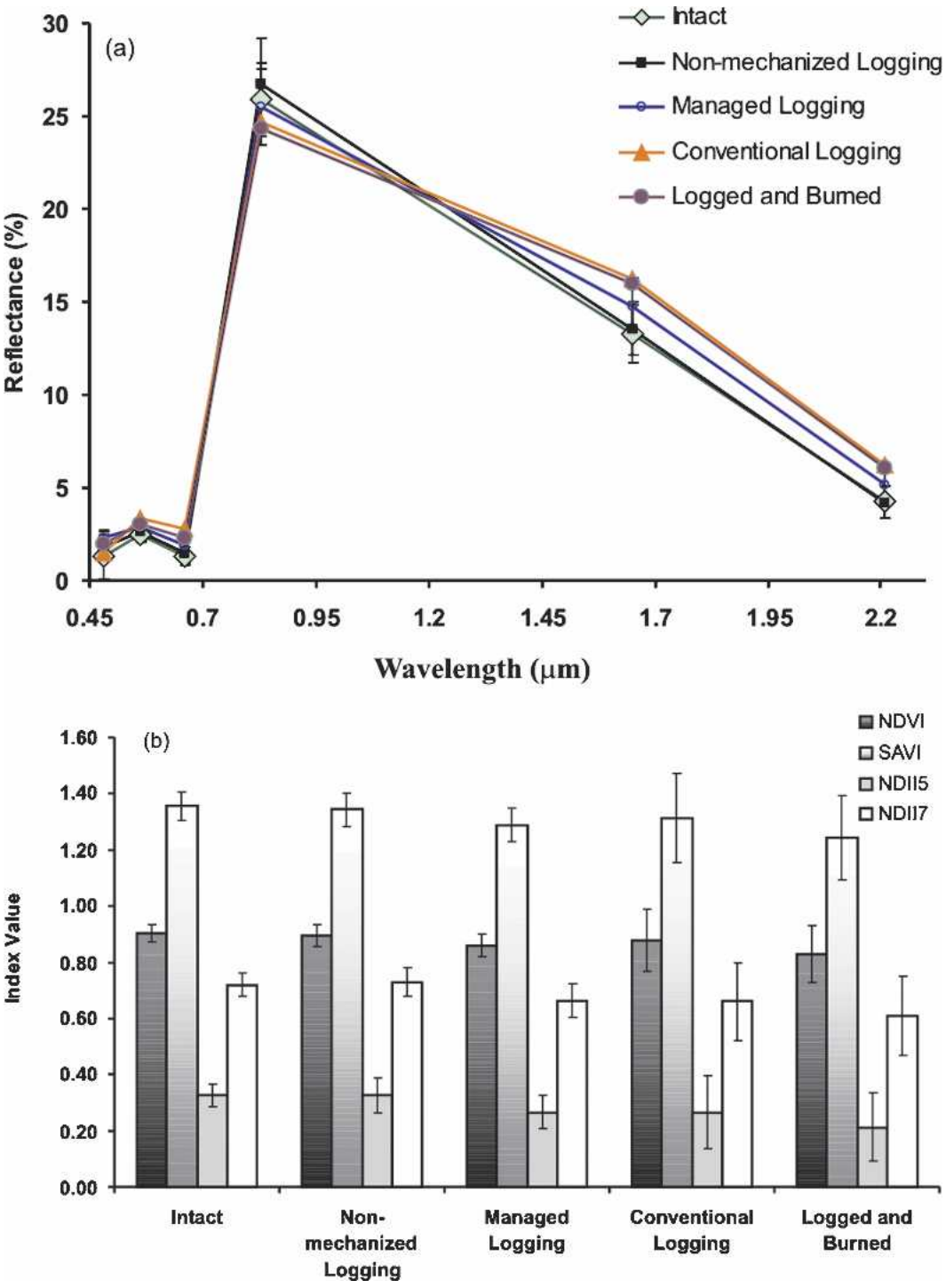

Figure 2. Means and standard deviations (vertical error bar) of intact forest and degraded forest classes as measured by Landsat bands: (a) reflectance, (b) vegetation and infrared indices, and (c) fraction images.

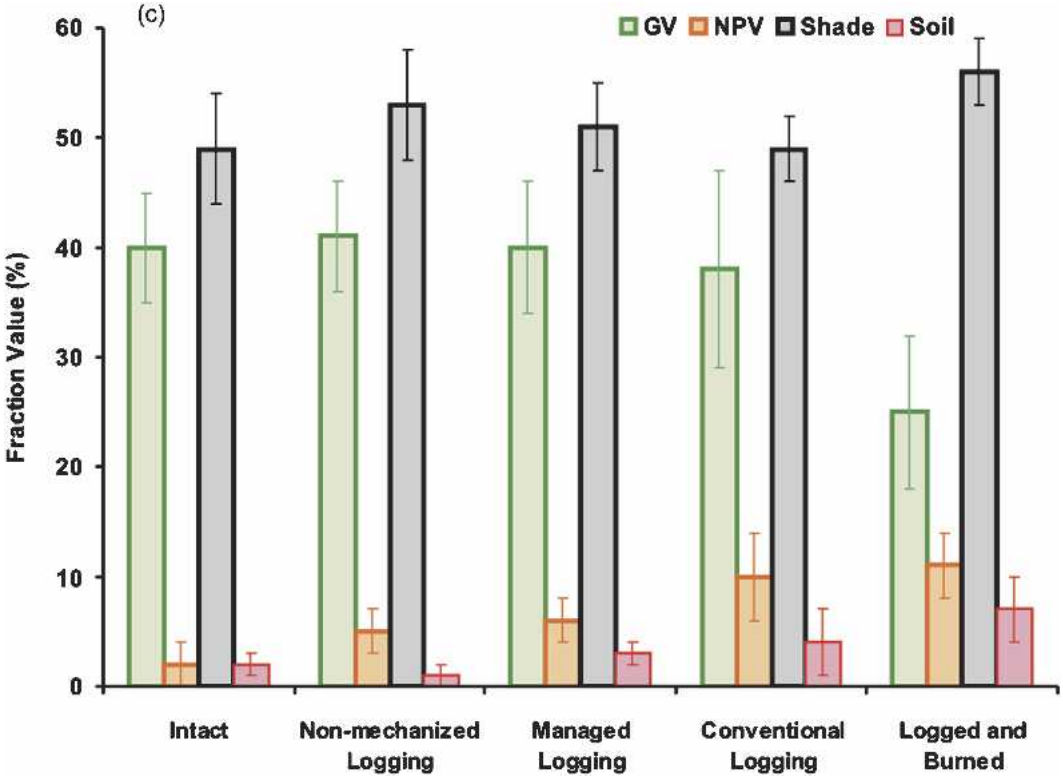

Figure 2. (*Continued*)

significant differences from intact forest and from each other with the Tukey test (Table 4).

5.1.3. Fraction images

The green vegetation (GV) fraction was not significantly different between intact forest and nonmechanized logging and managed logging. These three classes, however, were significantly different from conventional logging and logged and burned (Figure 2c). Conventional logging and logged and burned could also be separated from each other with the GV fraction. The NPV soil and shade fractions showed results similar to the GV fraction, except that the shade fraction showed a significant difference between intact forest and nonmechanized logging, and soil showed a significant difference between intact forest and managed logging (Table 4; Figure 2c).

The fraction images showed a higher absolute change between intact forest and the forest degradation classes (Figures 2c and 3c) when compared to the changes detected by the reflectance bands and the vegetation and infrared indices (Figures 2a,b; Figures 3a,b). The GV fraction decreased nonlinearly with degradation intensity (Figure 3c). A significant change in mean of about 3% was observed between intact forest and conventional logging class and of 15% between intact forest and logged and burned (Figure 3c; Table 4).

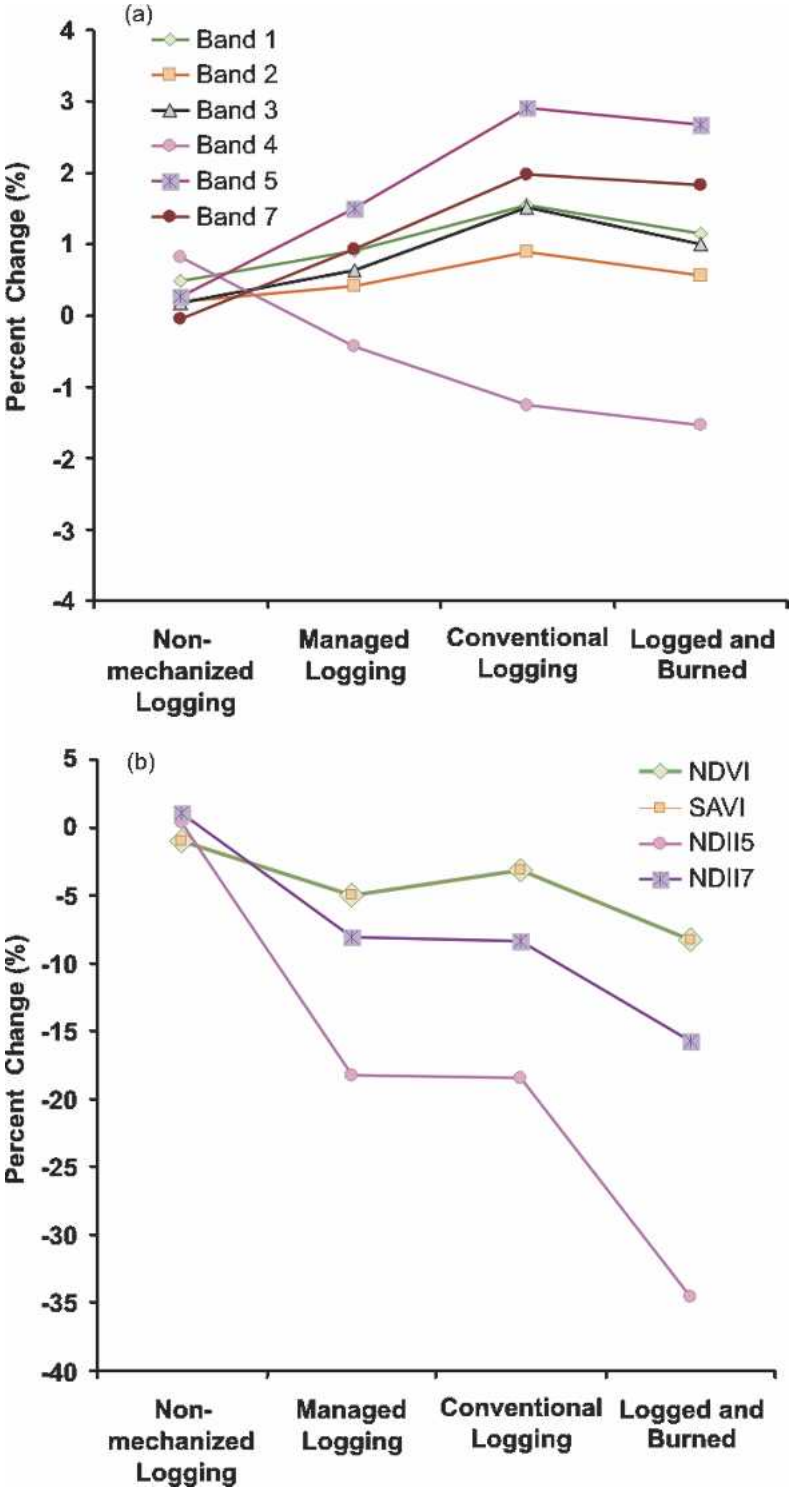

Figure 3. Delta change of (a) reflectance, (b) vegetation and infrared indices, and (c) fraction images, computed by subtracting the mean value of intact forest from the mean value of each degraded forest class.

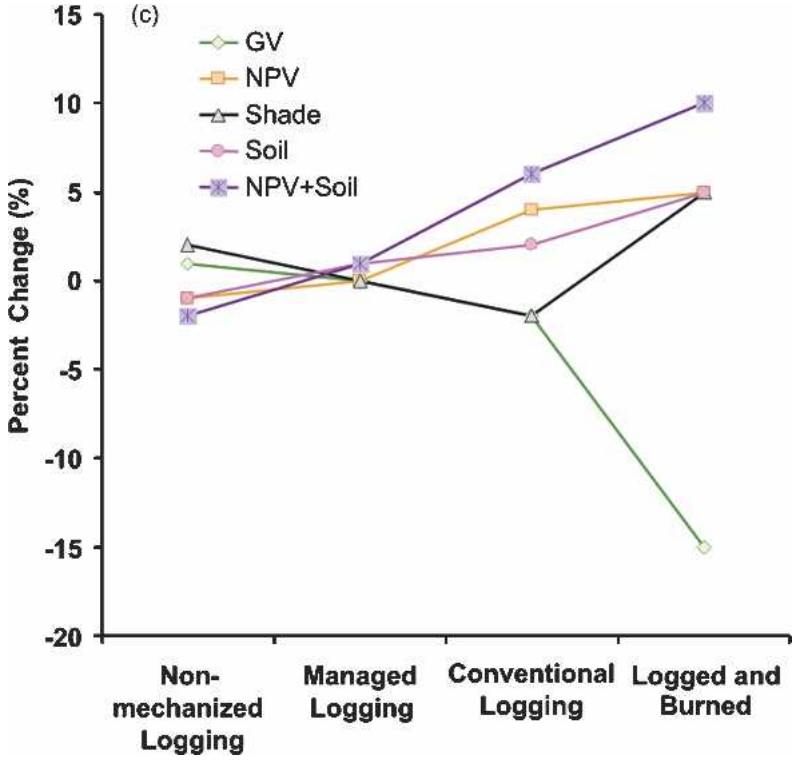

Figure 3. (*Continued*)

The shade fraction changed less than 5% from intact forest to the most degraded forest class, logged and burned. Changes in means and statistically significant differences were observed in NPV for the conventional logging and logged and burned classes. The mean NPV fraction increased by about 5% between the intact forest and the conventional logging classes, and between the intact forest and logged and burned classes (Figure 3c; Table 4). The soil fraction showed a similar change, but it was smaller than the change exhibited by the NPV fraction. When NPV and soil are combined, the changes between intact forest and the degraded forest classes become much greater (Figure 3c).

5.2. Multiyear forest degradation separability

The temporal analyses covered the year prior to the degradation process (i.e., intact forest; time = 0) up to 4 yr after the degradation process (time = 1, . . . , 4). Time represents the number of years after the last forest degradation event took place. Finally, the boldface mean values in Table 4 indicate statistically significant changes from the intact forest condition (time = 0) relative to any other year (time = 1, . . . , 4) obtained with the Tukey test.

5.2.1. Reflectance and indices

Two years after degradation, nonmechanized logging showed an increase in mean reflectance in the visible and infrared regions, significantly different from the

Table 4. Means and standard deviations of fractions, reflectance, and indices of forest degradation classes through time. Age zero means the year prior to the degradation process when the forest was under intact condition. Means presented with standard deviation noted parenthetically. Numbers in boldface denote significant differences between intact forest (time = 0) and degraded forest classes (time = 1, . . . , 4) at $P < 0.01$ utilizing a Tukey test.

Time	GV	NPV	Soil	Shade	B1	B2	B3	B4	B5	B7	NDVI	SAVI	NDII5	NDII7
	(%)	(%)	(%)	(%)	(%)	(%)	(%)	(%)	(%)	(%)				
(a) Class: Nonmechanized logging														
0	39	8	2	52	0.63	2.52	1.38	25.93	13.33	4.27	0.90	1.35	0.32	0.72
	(5)	(2)	(1)	(4)	(2.1)	(0.5)	(0.5)	(2.3)	(1.4)	(0.7)	(0.03)	(0.05)	(0.04)	(0.04)
1	41	**6**	3	53	**1.83**	2.64	1.47	26.74	13.55	4.20	0.90	1.34	0.33	0.73
	(5)	(3)	(2)	(5)	(0.6)	(0.5)	(0.5)	(2.4)	(1.4)	(0.9)	(0.04)	(0.06)	(0.06)	(0.05)
2	**43**	7	2	**48**	**2.36**	**3.31**	**1.84**	**28.64**	**14.07**	**5.07**	**0.88**	**1.32**	0.34	0.70
	(8)	(3)	(1)	(6)	(3.1)	(1.3)	(0.7)	(3.5)	(1.3)	(1.0)	(0.04)	(0.06)	(0.07)	(0.05)
3	**42**	**6**	3	50	0.63	2.54	1.20	26.19	13.72	4.45	0.91	1.37	0.31	0.71
	(5)	(2)	(1)	(4)	(2.0)	(0.3)	(0.6)	(2.2)	(1.3)	(0.8)	(0.04)	(0.06)	(0.04)	(0.04)
4	**47**	**5**	1	**46**	1.28	2.63	1.39	**27.42**	13.44	4.37	0.90	1.36	0.34	0.73
	(6)	(2)	(1)	(7)	(0.5)	(0.7)	(0.7)	(2.2)	(1.4)	(0.6)	(0.04)	(0.06)	(0.04)	(0.03)
(b) Class: Managed logging														
0	40	5	2	50	1.62	2.70	1.47	27.01	13.41	4.26	0.90	1.34	0.34	0.73
	(2)	(3)	(1)	(3)	(0.5)	(0.3)	(0.4)	(1.4)	(1.2)	(0.6)	(0.03)	(0.04)	(0.04)	(0.04)
1	40	6	**3**	51	**2.26**	**2.87**	**1.92**	**25.49**	**14.77**	**5.16**	**0.86**	**1.29**	**0.27**	**0.66**
	(6)	(2)	(1)	(4)	(0.5)	(0.4)	(0.5)	(2.1)	(1.5)	(0.9)	(0.04)	(0.06)	(0.06)	(0.06)
2	**47**	6	2	**45**	1.66	2.66	1.53	**25.97**	13.76	4.61	0.89	1.33	0.31	0.70
	(6)	(2)	(1)	(5)	(0.7)	(0.5)	(0.6)	(1.9)	(1.3)	(0.7)	(0.04)	(0.06)	(0.05)	(0.05)
3	**48**	5	**3**	**45**	**1.09**	2.49	1.41	26.53	13.47	4.54	0.90	1.35	0.33	0.71
	(4)	(2)	(1)	(3)	(0.5)	(0.6)	(0.7)	(1.6)	(1.7)	(0.8)	(0.05)	(0.07)	(0.05)	(0.05)
4	40	6	**3**	50	1.51	2.88	1.80	26.26	13.38	4.44	0.87	1.31	0.33	0.71
	(5)	(2)	(1)	(4)	(0.4)	(0.5)	(0.5)	(1.8)	(1.5)	(0.8)	(0.03)	(0.05)	(0.05)	(0.04)
(c) Class: Conventional logging														
0	45	3	2	50	1.72	2.11	0.98	24.62	12.72	3.92	0.92	1.38	0.33	0.73
	(3)	(2)	(1)	(3)	(0.7)	(0.3)	(0.5)	(2.1)	(1.1)	(0.7)	(0.02)	(0.04)	(0.05)	(0.05)
1	**38**	**10**	**4**	**52**	**1.50**	**3.34**	2.80	24.65	**16.19**	6.21	**0.88**	**1.31**	**0.27**	**0.66**
	(9)	(4)	(3)	(4)	(1.9)	(1.3)	(1.8)	(2.8)	(3.6)	(2.6)	(0.11)	(0.16)	(0.13)	(0.14)
2	**38**	**5**	3	**54**	0.62	**2.63**	1.70	25.66	**14.36**	**4.95**	0.89	1.34	0.31	0.70
	(7)	(2)	(2)	(5)	(1.9)	(0.6)	(0.9)	(2.9)	(2.4)	(1.5)	(0.05)	(0.08)	(0.06)	(0.07)
3	**35**	**8**	3	**54**	**1.08**	2.33	1.42	25.87	13.48	4.42	0.92	1.37	0.34	0.73
	(6)	(2)	(2)	(5)	(0.5)	(0.7)	(0.8)	(2.7)	(2.0)	(1.5)	(0.05)	(0.07)	(0.06)	(0.07)
4	**41**	**5**	3	52	**2.45**	2.58	1.56	**26.66**	13.99	4.85	**0.87**	**1.31**	0.30	0.69
	(5)	(2)	(1)	(4)	(0.4)	(0.6)	(0.8)	(2.6)	(2.1)	(1.3)	(0.03)	(0.05)	(0.04)	(0.05)
(d) Class: Logged and burned														
0	37	5	1	57	1.40	2.46	1.33	26.10	13.66	4.50	0.90	1.36	0.32	0.71
	(5)	(2)	(2)	(4)	(1.9)	(0.5)	(0.7)	(2.1)	(2.4)	(1.5)	(0.04)	(0.06)	(0.07)	(0.07)
1	**25**	**11**	**7**	**56**	**1.95**	**3.01**	**2.29**	**24.38**	**15.96**	**6.06**	**0.83**	**1.24**	**0.21**	**0.61**
	(7)	(3)	(3)	(3)	(1.1)	(0.8)	(1.4)	(2.3)	(3.4)	(2.6)	(0.10)	(0.15)	(0.12)	(0.14)
2	36	**8**	**5**	**51**	**2.72**	**3.32**	**2.84**	**23.36**	**17.73**	7.41	**0.78**	**1.17**	**0.14**	**0.52**
	(4)	(2)	(2)	(3)	(0.5)	(0.6)	(0.9)	(2.9)	(2.7)	(2.0)	(0.08)	(0.12)	(0.10)	(0.12)
3	**51**	**8**	**2**	**40**	**1.88**	**2.83**	**1.82**	**26.59**	**16.41**	**5.91**	**0.87**	**1.30**	**0.24**	**0.63**
	(5)	(2)	(1)	(4)	(0.6)	(0.4)	(0.6)	(3.5)	(2.1)	(1.0)	(0.05)	(0.07)	(0.07)	(0.07)
4	**48**	**6**	**3**	**43**	**1.14**	**2.64**	1.50	28.62	**15.48**	5.16	0.90	1.35	0.30	0.69
	(5)	(2)	(1)	(5)	(0.5)	(0.6)	(0.7)	(3.3)	(1.8)	(0.7)	(0.05)	(0.07)	(0.04)	(0.04)

intact forest mean reflectance (Table 4a). This increase in reflectance generated changes in the vegetation and infrared indices in the second year, but only the changes in means of NDVI and SAVI were statistically significant for nonmechanized logging in the second year. No significant change in reflectance and in the indices was observed for the third and fourth years in nonmechanized logging, except for band 4, which showed a significant increase (Table 4a).

Managed logging showed only two significant temporal changes in mean reflectance for bands 1 and 4, in the third and second years (Table 4b). Neither the vegetation indices nor the infrared indices showed temporally significant changes in mean values according to the Tukey test results for managed logging (Table 4b).

The logging class showed some significant temporal changes in mean reflectance and mean index values. Bands 2, 3, 5, and 7 showed significant differences from intact forest 2 yr after logging took place (Table 4c). Significant differences were observed in bands 1 and 4, for 3 and 4 yr after logging, as a result of an increase in mean values that might be associated with forest regeneration. Finally, only the vegetation indices showed significant changes due to logging disturbance for the fourth year (Table 4c).

Changes in logged and burned areas were significant for most of the reflectance bands for all the years following the degradation process. Among the indices, only NDII5 showed a significant difference between intact forest and logged and burned in the fourth year (Table 4d).

5.2.2. Fraction images

Nonmechanized logging showed a significant increase in GV mean from the intact forest mean in the second, third, and fourth years after logging. A significant decrease in NPV mean, relative to the intact forest mean, occurred in the third and fourth years for this class. The shade fraction showed a significant decrease in mean in the second and fourth years (Table 4a).

Managed logging showed a significant change between intact forest and nonmechanized logging for the GV fraction in the second and fourth years. The results indicate that no significant change in GV and shade means occurred in the first year, when the degradation took place. However, an increase in GV and a decrease in shade were observed in the second and third years, which is likely to be associated with forest canopy closure after logging. The NPV fraction, however, did not show any significant change between intact forest and managed logging for all the years. Finally, soil and shade fractions were significantly different between these two classes for all the years (Table 4b).

The conventional logging class showed a significant difference in mean for GV, NPV, and shade fractions for all the years. The soil fraction was significantly different from intact forest only in the first year (Table 4c).

The logged and burned class is affected by two degradation processes—selective logging and burning. Because these are heavily degraded forest environments, significant changes in all fractions were revealed with the Tukey test (Table 4c). Mean GV fraction decreased after burning followed by an increase in GV mean in the following years. The NPV mean showed an opposite pattern compared to GV mean, with an increase in mean in the first year followed by a decrease in NPV mean in the subsequent years. In the second year after burning, the shade

fraction became important for distinguishing intact forest from logged and burned forest because of a decrease in mean value (Table 4c).

5.3. Optimal temporal resolution

Nonmechanized logging is more difficult to distinguish from intact forest than the other types of disturbances in the first year. Green vegetation and shade fractions varied inversely over time for this class (i.e., an increase in GV is followed by a decrease in shade; Figure 4a). Because this type of selective logging does not greatly impact the forest in the year when the forest disturbance took place, the significant changes observed might be associated with canopy closure after logging. Therefore, the optimal temporal resolution for detecting this type of logging is between 2 and 3 yr, when canopy closure is more likely to happen, reducing canopy roughness and, as a result, decreasing shade content. But, because this type of low impact logging does not build roads and log landings, its differentiation from other types of disturbances (e.g., blow down winds) becomes much harder using the forest regeneration signal.

Managed logging is more likely to be detected with reflectance bands and vegetation and infrared indices in the first year. The soil fraction was the only SMA result that showed significant change in the first year for this class. However, a higher magnitude change in GV and shade fractions means were observed in managed logging when compared with the changes observed in nonmechanized logging (Figures 4a,b). Therefore, the regeneration of managed forests is more likely to be detected in the second and third years than the actual low disturbance in the first year. In addition, the roads and log landing built in managed forests can be used to differentiate managed logging from other types of forest disturbances. After the fourth year, no change relative to intact forest can be observed.

Conventional logging and logged and burned areas can be detected in the first year with all reflectance bands, indices, and fractions. However, regeneration changes in the conventional logging areas, in the subsequent years, are more likely to be detected using fraction images. The conventional logging class can be distinguished from intact forest in the first year because of a decrease in GV and an increase in NPV (Figure 4c). After the second year, an increase in GV and decrease in NPV is observed. However, our temporal time series shows a second decrease in GV and an increase in NPV means in the third year (Figure 4c). Such a pattern may be due to a second harvesting operation (recurrent logging), which is common in the study area. The temporal fraction pattern of logged and burned areas shows a more dramatic decrease in GV and an increase in NPV mean values in the first year after degradation (Figure 4d). The NPV signal is still high in the second year, and after the third year, GV increases and NPV decreases. Therefore, the optimal temporal resolution for detecting disturbances in conventional logging and logged and burned environments is 1 yr; regeneration, however, can be detected in logged and burned areas up to 4 yr.

The time series results indicate that intensive and unplanned logging, and logging followed by burning, can be detected in the first year. Up to the second year, detection becomes a challenge because of forest regeneration. Less intensive forest impacts, such as those caused by nonmechanized logging and managed logging are more difficult to detect even in the year after degradation took place. The regen-

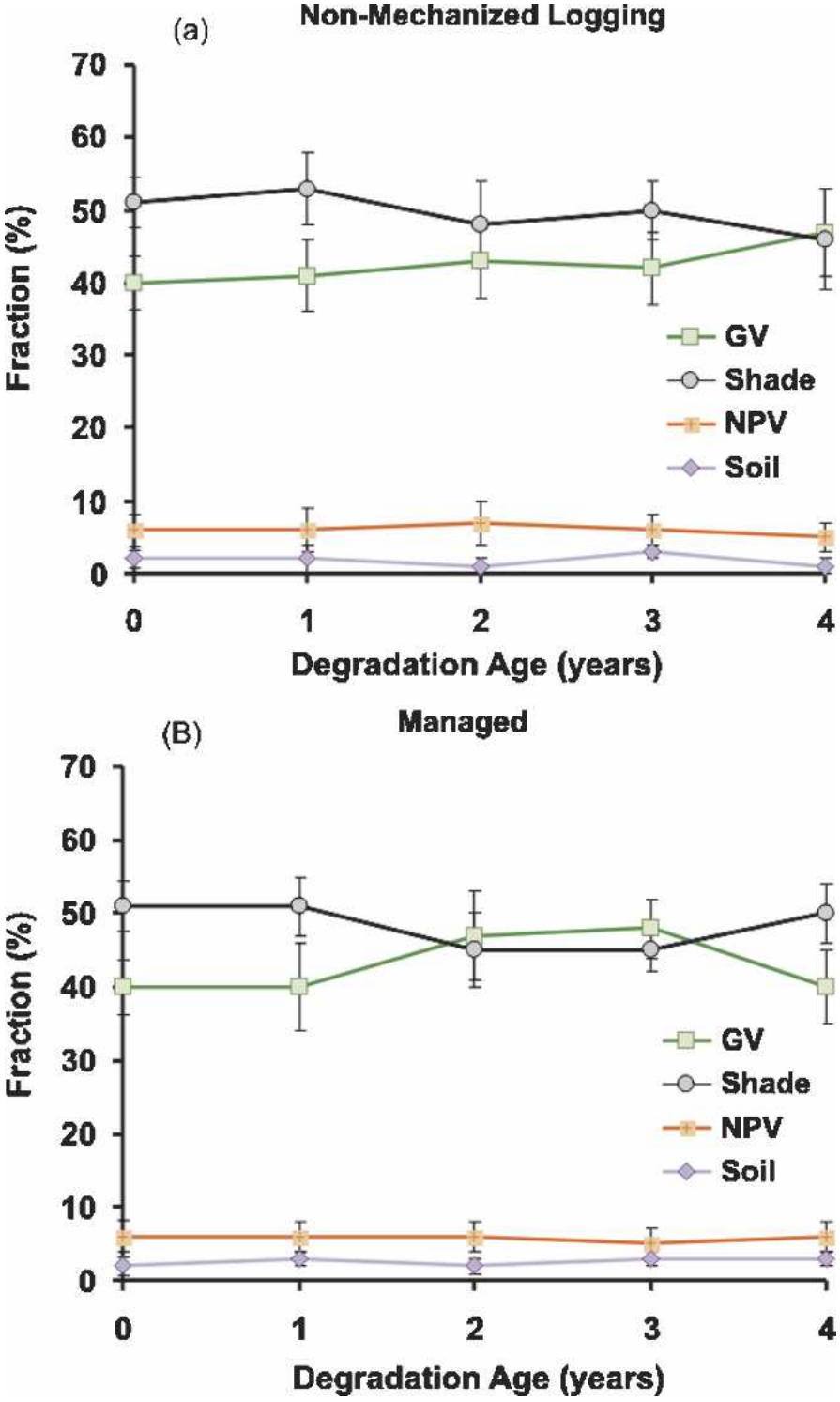

Figure 4. Change in mean fraction values through time for (a) nonmechanized logging, (b) managed logging, (c) conventional logging, and (d) logged and burned.

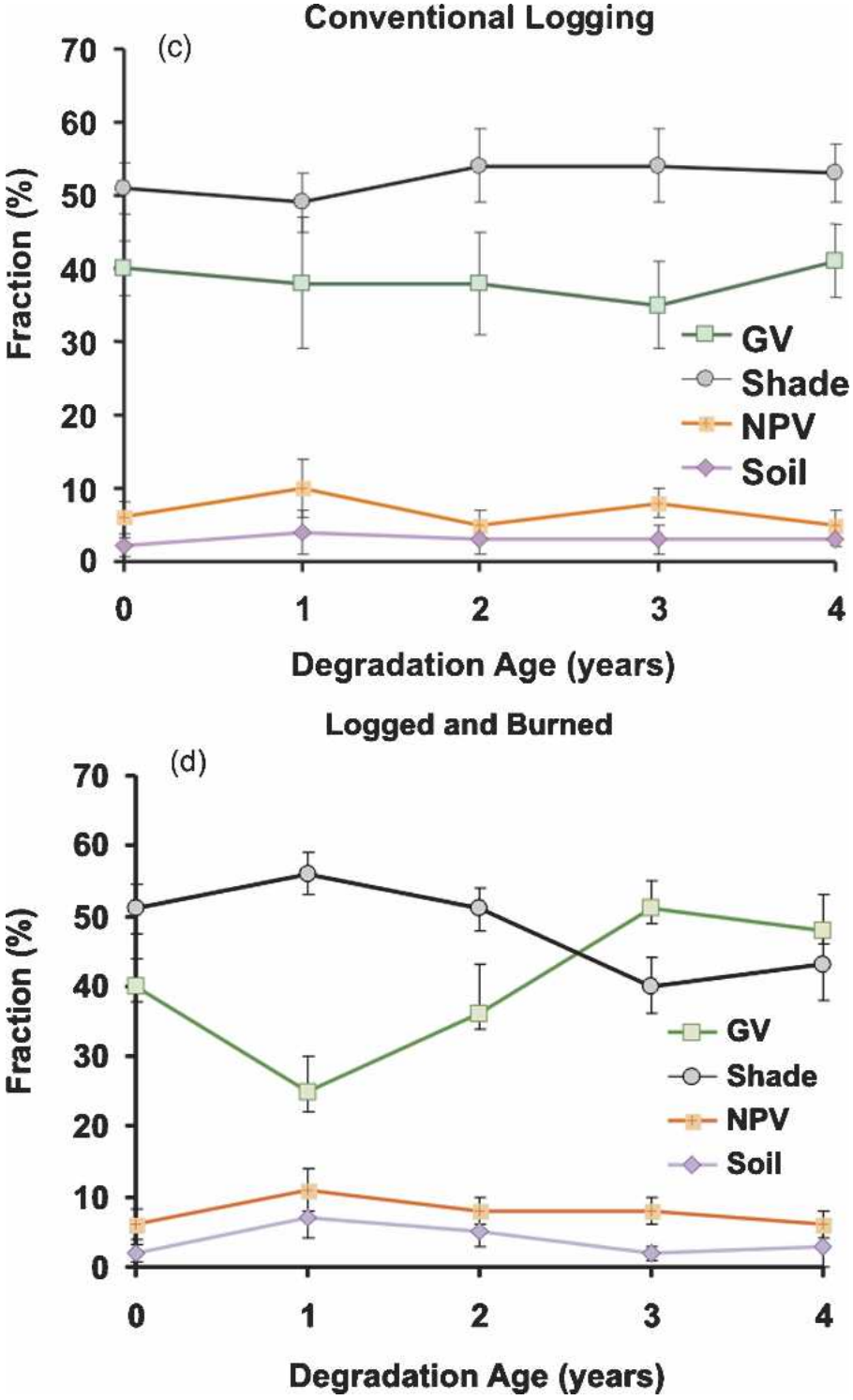

Figure 4. (*Continued*)

eration signal of these low-intensity types of logging becomes significant in the second and third years. But, the detection of logging infrastructure is important to distinguish this low-impact logging from other types of forest disturbance.

6. Discussion

6.1. Degraded forest mapping potential

The fraction images derived from SMA have more advantages in differentiating types of degraded forests than reflectance data and vegetation and infrared indices. First, the fraction images showed higher absolute changes in mean values between intact forest and the other degraded forest classes than the other types of data. Second, the statistical comparisons are more temporally consistent using the fraction images. Third, the fraction contents have a more intuitive physical link with field data. Additionally, fraction images have been successfully used to map selective logged and burned forest areas. For example, Cochrane and Souza (Cochrane and Souza 1998) reported that the NPV fraction showed the greatest separability of subclasses of burned forests and Souza et al. (2003) demonstrated that the NPV fraction was an important variable for differentiating intact forest from degraded forest in a decision tree classifier. Finally, other studies have shown that damage associated with selective logging is difficult to identify and map using Landsat reflectance data (Stone and Lefebvre 1998; Asner et al. 2002).

Fraction temporal changes revealed in the statistical comparisons described above can be observed visually using a color composite of fraction images (Figure 5). When displaying NPV, GV, and soil as blue, green and red, respectively, we can identify and potentially map degraded forest classes. NPV is the most prominent fraction change in the degraded forest environment and is easily observed in this type of color composite.

One important issue that should be taken into consideration when interpreting forest degradation signatures in this type of color composite is the time of image acquisition versus the time when the degradation event took place. For example, the managed logging areas of transects 15 and 17 do not exhibit an NPV signature in 1999, because no selective logging had taken place in that year (Figure 5a). In the following year, only transect 15 showed an increase in NPV due to selective logging, but no increase in NPV was observed in transect 17 (Figure 5b). To explain why this is possible, one must consider the time of both harvesting and image acquisition. The Landsat image for the year 2000 was acquired immediately after harvesting took place in the area of transect 15 but before harvesting occurred near transect 17 (Figure 5b). In the next image, acquired in 2001, the NPV signal in transect 15 area is no longer as visible, but the NPV content has increased in transect 17 relative to the images acquired in 1999 and 2000. This type of temporal lag between image acquisition and harvesting is important for building change detection classifiers for mapping degraded forest.

The NPV fraction signature was more visible and persistent in logged and burned environments (Figures 5e–h). In the area of transects 3, 4, and 5, selective logging took place in 1999 followed by intensive forest burning in 2000. NPV increased more drastically in burned areas, and its signature was still visible in

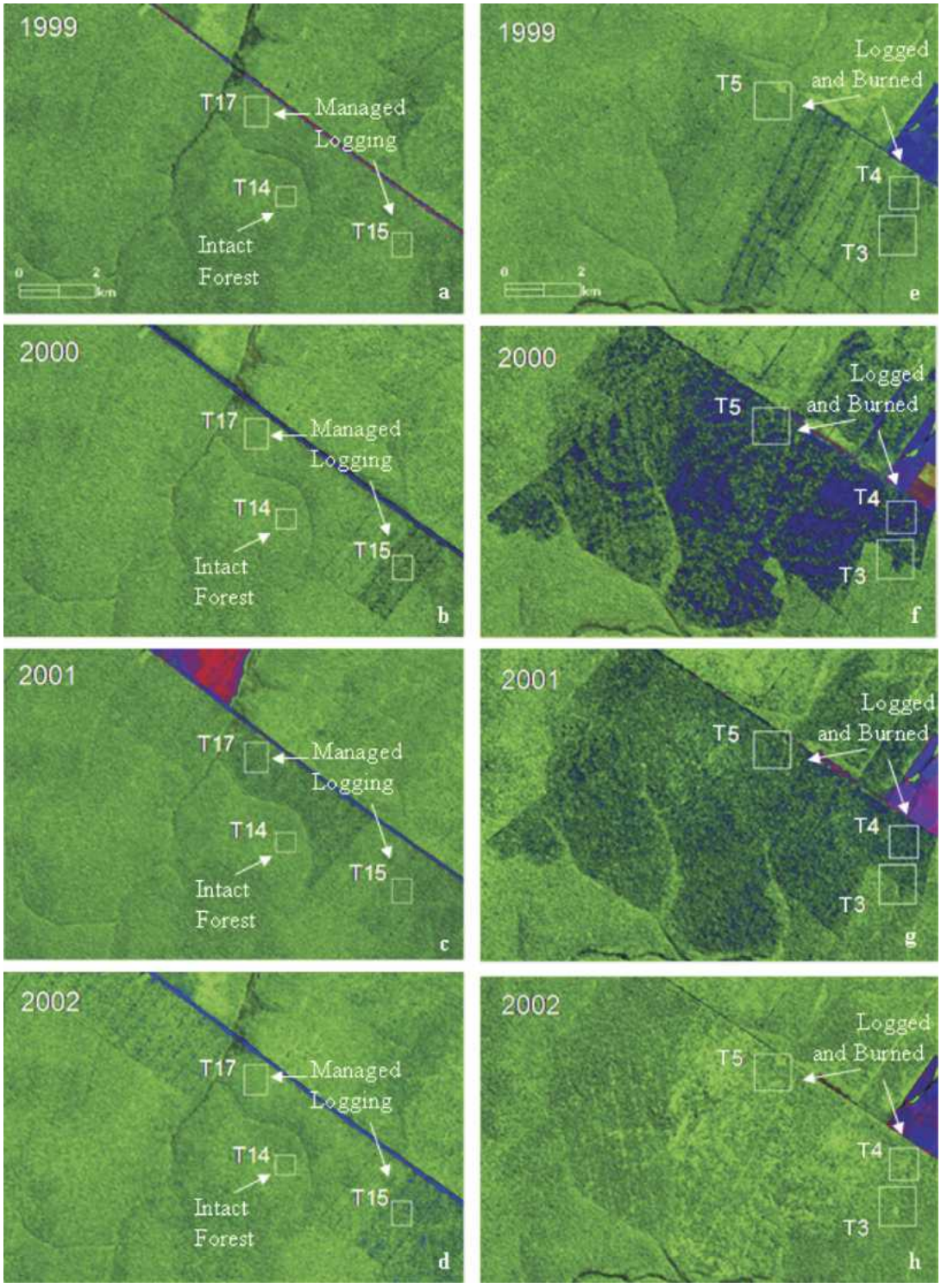

Figure 5. Examples of forest degradation processes and temporal changes as detected using fraction images derived from SMA (red: soil, green: GV, and blue: NPV).

2001. In 2002, the NPV signature disappeared, followed by an increase in GV and a decrease in shade.

6.2. Linking field measurements with fraction images

Forest biophysical properties acquired with the forest transect for intact forest and the degraded forest classes are summarized in Table 5. The results obtained with the SMA agree with the field measurements. The GV fraction tends to decrease as a function of degradation intensity. At the field scale, this change in GV can be explained by a decrease in the amount of intact vegetation and canopy cover. Our field results show that the mean of intact vegetation proportion drops from 95% in the intact forest to 50% in logged and burned areas (Figure 2c; Table 5). The canopy cover also decreased from intact forest (93%) to logged and burned (67%).

The proportion of the forest area affected by disturbed soil and wood debris tends to increase as a function of the degradation intensity. This pattern also agrees with the pattern captured by soil and NPV fractions (Figure 2c; Table 5). At the field level, all these ground disturbances are significant for differentiating intact forest from the degradation classes. However, because the ground cover is not always imaged by satellite sensors, the distinction of these classes from Landsat is not always possible using these field properties.

NPV fraction has an inverse relationship with biomass measurements made in degraded forests in the eastern Amazon (Souza et al. 2003). In our study area, the biomass estimates obtained with the field transects also show a trend in decreasing biomass with an increase in NPV as a function of degradation intensity (Figure 2c; Table 5). Even though it is not the objective of this paper to evaluate if these correlations are statistically significant, the results indicate that there is a potential for using the NPV fraction images to estimate biophysical properties of degraded forests in open forest environments as well.

6.3. Monitoring forest degradation: Practical application and challenges

One potential application of the fraction change detection technique presented in this study is the discrimination between managed and unplanned logging. Cur-

Table 5. Estimation of forest biophysical properties based on forest transects. Means presented with the standard deviation noted parenthetically. Different letters denote significant differences among degradation classes at $P < 0.05$ utilizing a Tukey test.

Biophysical property	Intact ($n = 4$)	Nonmechanized logging ($n = 5$)	Managed logging ($n = 5$)	Conventional logging ($n = 2$)	Logged and burned ($n = 3$)
Ground cover (%)					
Intact vegetation	95 (5)a	83 (9)ab	50 (11)c	59 (3)bc	50 (19)c
Woody debris	4 (5)a	10 (11)ab	29 (7)ab	17 (8)ab	39 (28)b
Disturbed soil	0a	7 (2)ac	17 (6)bc	24 (12)b	5 (7)ac
Canopy cover (%)	93 (5)ab	87 (4)b	97 (1)a	92 (0)ab	67 (5)c
Aboveground live biomass (t ha^{-1})	306 (44)a	250 (20)a	219 (31)b	277 (44)a	166 (45)b

rently, there is an increasing need to monitor areas under forest management in the Amazon region. First, the Brazilian government has improved the control of selective logging in the region by requesting detailed information on the location of forest plots that will be subject to timber harvesting and requiring specific management practices following logging (Casa Civil 2004). Second, the logging private sector has become more interested in forest certification, which requires high standard management practices (Lentini et al. 2003). Finally, the Brazilian government has been evaluating the possibility of providing long-term concessions in national forest areas for logging companies interested in timber harvesting (Veríssimo et al. 2002). Therefore, low cost, timely, and reliable information on forest disturbances is required to monitor the forest areas authorized by the government and/or certified for conducting forest management.

The fraction change technique presented in this paper has the potential to be used to indicate if an area is following the management practices required by the Brazilian government and/or by the certification institutes. For example, both the GV and NPV fractions showed significant differences from intact forest to managed logging, but showed higher significant differences, and more pixels showed changes in fraction values from intact forest to conventional logging and logged and burned areas. In other words, the fraction change technique has the potential for differentiating managed logging areas from unplanned logging areas. Therefore, a forest monitoring program could use the fraction change technique to verify if the areas that have received government authorization and/or forest certification to manage forest areas for timber harvesting are following the management prescriptions.

There are, however, two main challenges to implementing a remote sensing program for monitoring forest management plans in the Amazon region. The first has to do with technical remote sensing issues. Reflectance retrieval, radiometric intercalibration, and SMA, particularly dealing with the need to find the correct set of end members, are not trivial tasks. Second, processing and interpreting the fraction data requires training the end users that will be in charge of such a forest-monitoring system.

7. Conclusions

Statistical multitemporal analysis of reflectance, vegetation, and infrared indices and fraction images, derived from SMA, showed that fraction images are more sensitive to changes in transitional forest environments due to selective logging and burning than the broadband indices tested here. Low intensity logging, such as managed logging and nonmechanized logging, are more difficult to distinguish from intact forest, but a regeneration signal—caused by understory vegetation growth and canopy closure—becomes significant in the second and third year due to an increase in GV and a decrease in shade. Our time series results showed that changes in GV and NPV fractions were higher when intact forest was changed to conventional logging and to logged and burned environments in the first year following the degradation event. In the logged and burned forests, the NPV signal was more persistent, showing a burned signature through the second year after forest burning. Therefore, both GV and NPV have the potential for use in change-

detection classifiers for identifying and mapping conventional logging and logged and burned forests in the Brazilian Amazon, with images no more than 1 yr apart.

Acknowledgments. The authors thank the PPG7—"Programa de Pesquisa Dirigida" (MMA/MCT/FINEP) for financial support provided to the Instituto do Homem e Meio Ambiente da Amazônia—Imazon for acquiring the Landsat images, and the Ford Foundation for supporting the work of André Monteiro. We also thank the NASA LBA-ECO Phase 2 Research Program for funding this project. Finally, we thank Frank Pantoja and Josieldo Pantoja for field assistance during forest inventories.

References

Adams, J. B., M. O. Smith, and A. R. Gillespie, 1993: Imaging spectroscopy: Interpretation based on spectral mixture analysis. *Remote Geochemical Analysis,* C. M. Englert and P. A. J. Englert, Eds., Topics in Remote Sensing, Vol. 4, Cambridge University Press, 145–166.

Asner, G. P., M. Keller, R. Pereira, and J. C. Zweede, 2002: Remote sensing of selective logging in Amazonia: Assessing limitations based on detailed field observations, Landsat ETM+ and textural analysis. *Remote Sens. Environ.,* **80,** 483–492.

——, ——, ——, ——, and J. Silva, 2004: Canopy damage and recovery after selective logging in Amazonia: Field and satellite studies. *Ecol. Appl.,* **14,** s280–s298.

Boardman, J. W., F. A. Kruse, and R. O. Green, 1995: Mapping target signatures via partial unmixing of AVIRIS data. *Summaries of the Fifth Airborne Earth Science Workshop,* JPL Publication 95, Pasadena, CA, Jet Propulsion Laboratory, 23–26.

Casa Civil, 2004: Plano de ação para a prevenção e controle do desmatamento na Amazônia legal. Relatório da Presidência da República, Casa Civil, 156 pp. [Available online at http://www.amazonia.org.br/arquivos/101504.pdf.]

Cochrane, M. A., and C. Souza Jr., 1998: Linear mixture model classification of burned forests in the eastern Amazon. *Int. J. Remote Sens.,* **19,** 3433–3440.

——, and M. D. Schulze, 1999: Fire as a recurrent event in tropical forests of the eastern Amazon: Effects on forest structure, biomass, and species composition. *Biotropica,* **31,** 2–16.

——, A. Alencar, M. Schulze, C. Souza Jr., D. Nepstad, P. Lefebvre, and E. Davidson, 1999: Positive feedbacks in the fire dynamic of closed canopy tropical forest. *Science,* **284,** 1832–1835.

Furby, S. L., and N. A. Campbell, 2001: Calibrating images from different dates to 'like-value' digital counts. *Remote Sens. Environ.,* **77,** 186–196.

Gerwing, J., 2002: Degradation of forests through logging and fire in the eastern Brazilian Amazon. *For. Ecol. Manage.,* **157,** 131–141.

Hogg, R. V., and A. Craig, 1995: *Introduction to Mathematical Statistics.* 5th ed. Prentice Hall, 576 pp.

Holdsworth, A. R., and U. C. Uhl, 1997: Fire in Amazonian selectively logged rain forest and the potential for fire reduction. *Ecol. Appl.,* **7,** 713–725.

Huete, A. R., 1988: A soil-adjusted vegetation index (SAVI). *Remote Sens. Environ.,* **25,** 295–309.

Hunt, E. R., and B. N. Rock, 1989: Detection of changes in leaf water content using near and middle-infrared reflectances. *Remote Sens. Environ.,* **30,** 43–54.

INPE, cited 2003: Monitoramento da floresta Amazônica Brasileira por satélite 1999–2001. Instituto Nacional de Pesquisas Espaciais. [Available online at http://www.dpi.inpe.br/prodesdigital.]

Johns, J. S., P. Barreto, and C. Uhl, 1996: Logging damage during planned and unplanned logging operations in the eastern Amazon. *For. Ecol. Manage.,* **89,** 59–77.

Lambin, E. F., 1999: Monitoring forest degradation in tropical regions by remote sensing: Some methodological issues. *Global Ecol. Biogeogr.,* **8,** 191–198.

Lentini, M., A. Veríssimo, and L. Sobral, 2003: Forest facts in the Brazilian Amazon 2003. Imazon, 108 pp. [Available online at http://www.imazon.org.br/upload/forest_facts_2003_v4a.pdf.]

Martini, A., N. Rosa, and C. Uhl, 1994: An attempt to predict which Amazonian tree species may be threatened by logging activities. *Environ. Conserv.,* **21,** 152–162.

Monteiro, A. L., C. Souza Jr., and P. Barreto, 2003: Detection of logging in Amazonian transition forest using spectral mixture models. *Int. J. Remote Sens.,* **1,** 151–159.

——, ——, ——, F. Pantoja, and J. Gerwing, 2004: Impactos da exploração madeireira e do fogo em florestas de transição da Amazônia Legal. *Sci. For.,* **65,** 11–21.

Nepstad, D., and Coauthors, 1999: Large-scale impoverishment of Amazonian forests by logging and fire. *Nature,* **398,** 505–508.

Ott, L., 1992: *An Introduction to Statistical Methods and Data Analysis.* 4th ed. Duxbury Press, 1051 pp.

RADAMBRASIL, 1981: Projeto Radam Brasil, Levantamento de Recursos Naturais. Departamento de Produção Mineral, Folha SC.21 Juruena, Vol. 20, Rio de Janeiro, Brazil, 30–40.

Roberts, D. A., G. T. Batista, J. L. G. Pereira, E. K. Walker, and B. W. Nelson, 1998: Change identification using multitemporal spectral mixture analysis: Applications in eastern Amazonia. *Remote Sensing Change Detection: Environmental Monitoring Methods and Applications*, R. S. Luneetta and C. D. Elvidge, Eds., Ann Arbor Press, 137–159.

Rouse, J. W., R. H. Haas, J. A. Schell, D. W. Deering, and J. C. Harlan, 1974: Monitoring the vernal advancement and retrogradation (greenwave effect) of natural vegetation. NASA GSFC Type III Final Rep., Greenbelt, MD, 371 pp.

Sgrenzaroli, M., A. Baraldi, H. Eva, G. De Grandi, and F. Achard, 2002: Contextual clustering for image labeling: An application to degraded forest assessment in Landsat TM images of the Brazilian Amazon. *IEEE Trans. Geosci. Remote Sens.,* **40,** 1833–1848.

Souza, C., and P. Barreto, 2000: An alternative approach for detecting and monitoring selectively logged forests in the Amazon. *Int. J. Remote Sens.,* **21,** 173–179.

——, L. Firestone, L. Moreira Silva, and D. Roberts, 2003: Mapping forest degradation in the Eastern Amazon from SPOT 4 through spectral mixture models. *Remote Sens. Environ.,* **87,** 494–506.

Stone, T. A., and P. Lefebvre, 1998: Using multi-temporal satellite data to evaluate selective logging in Para, Brazil. *Int. J. Remote Sens.,* **19,** 2517–2526.

Verbyla, D. L., and S. H. Boles, 2000: Bias in land cover change estimates due to misregistration. *Int. J. Remote Sens.,* **21,** 3553–3560.

Veríssimo, A., M. A. Cochrane, and C. Souza Jr., 2002: National forests in the Amazon. *Science,* **297,** 1478.

Vidal, E., J. Johns, J. Gerwing, P. Barreto, and C. Uhl, 1997: Vine management for reduced-impact logging in the eastern Amazon. *For. Ecol. Manage.,* **98,** 105–114.

Watrin, O. S., and A. M. A. Rocha, 1992: Levantamento da vegetação natural e do uso da terra no Município de Paragominas (PA) utilizando imagens TM/Landsat. Research Bulletin 124, EMBRAPA/CPATU, Belém, Brazil, 40 pp.